The Tiber river delta plain (central Italy): Coastal evolution and implications for the ancient Ostia Roman settlement

P. Bellotti,[1] G. Calderoni,[1,2] F. Di Rita,[1] M. D'Orefice,[3] C. D'Amico,[4]
D. Esu,[1,2] D. Magri,[1] M. Preite Martinez,[1,2] P. Tortora[1] and P. Valeri[1]

Abstract

Geomorphologic, stratigraphic, faunistic, palynological and carbon isotope analyses were carried out in the area of the Tiber river mouth. The results depict a complex palaeoenvironmental evolution in the area of the Roman town of Ostia, ascertain the changes of the Tiber river delta over the last 6000 years and support a re-interpretation of some archaeologic issues. The wave-dominated Tiber delta evolved through three distinct phases. In the first step (5000–2700 yr BP) a delta cusp was built at the river mouth, which was located north of the present outlet. Subsequently (2700–1900 BP), an abrupt southward migration of the river mouth determined the abandonment of the previous cusp and the progradation of a new one. The third step, which is still in progress, is marked by the appearance of a complex cusp made up of two distributary channels. The transition from the first to the second evolution phase occurred in the seventh century BC and was contemporary to the foundation of Ostia, as suggested by historical accounts. However, the oldest archaeological evidence of the town of Ostia dates to the fourth century BC, when human activity is clearly recorded also by pollen data. We suggest that the first human settlement (seventh century BC) consisted of ephemeral military posts, with the aim of controlling the strategic river mouth and establishing the Ostia saltworks. Only after the fourth century BC the coastal environment was stable enough for the foundation and development of the town of Ostia.

Keywords

delta, geoarchaeology, geomorphology, Ostia, palaeoenvironment, sedimentology, Tiber

Introduction

The Tiber river delta plain is located some 25 km west of Rome in an area of great interest for the relationships between natural environmental changes and human activity, particularly during the Roman times. Recent works coupling archaeologic and geologic data have revived the debate on the history of this area (Bellotti et al., 2007; Giraudi, 2004; Giraudi et al., 2006; Goiran et al., 2007; Sadori et al., 2010). This study is aimed at gaining new insights into the evolution of the Tiber river delta plain, so improving the survey of the foundation and expansion of historical settlements in coastal areas, a subject of growing concern throughout the Mediterranean basin (Arnaud-Fassetta and Provansal, 1999; Arnaud-Fassetta et al., 2003; Blackmann, 2005; Fouache and Pavlopoulos, 2005; Marriner and Morhange, 2006, 2007; Morhange et al., 2003; Reinhardt et al., 1998; Stanley, 2005; Stanley and Bernasconi, 2006, 2009; Vella et al., 2005). In particular, the main objectives of this study are:

- to reconstruct the progression of the deltaic cusp of the Tiber river in the last few thousands of years;
- to define the changes of the vegetational landscape of the Tiber delta from the early Bronze age to the end of the Roman Empire;
- to assess timing and modes of the foundation of ancient Ostia by means of a multidisciplinary palaeoenvironmental approach,

and to compare the reconstructed dynamics with historical sources and archaeological evidence;
- to disentangle the role of natural versus man-induced processes in stabilizing the estuarine environment occupied by the Roman settlement of Ostia.

Study area

The Tiber river delta, a microtidal wave-dominated delta supplied by mud-sandy sediments (Galloway, 1975), stretches over some 25 km and includes a delta plain region and a submerged fan (Bellotti et al., 1994). The plain, which is composed of a flat inner portion with alluvial-marshy sediments and an outer strand-plain (Figure 1), formed during the Holocene, through the transition

[1]Università 'La Sapienza', Italy
[2]IGAG-CNR, Italy
[3]Servizio Geologico d'Italia, Italy
[4]Università del Molise, Italy

Corresponding author:
Piero Bellotti, Dipartimento di Scienze della Terra, Università 'La Sapienza', P.le A. Moro 5, 00185 Rome, Italy.
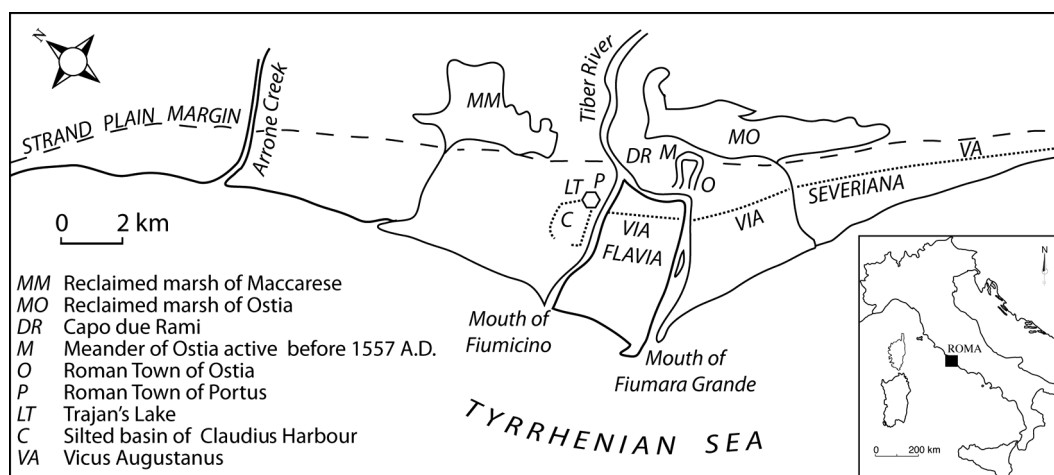Email: piero.bellotti@uniroma1.it

Figure 1. The Tiber river delta plain and the main Roman archaeological sites

from a former estuary (within the submerged Tiber river paleo-valley) to the present wave-dominated delta (Bellotti et al., 1995; Dalrymple et al., 1992; Roy et al., 2001). This evolution took place following three main stages: (i) estuary (mid-transgression) with a bay-head delta, a lagoon basin and discontinuous sandy ridges at the entrance of the estuary; (ii) wave-dominated estuary (late-transgression) consequent to the bay-head delta progradation splitting the former lagoon into two basins; (iii) wave-dominated delta (present highstand), following the formation of a bay-head barrier when the river mouth reached the sea; during this phase the modern strand-plain and the submarine fan originated and the final aggradation on the inner plain occurred.

This evolutionary trend implies that sediment deposition, formerly constrained into the narrow estuary basin, subsequently took place in the broad coast-shelf area. Changes in sediment input, climatic variations and, more recently, human activities played a major role in the development of the delta during the highstand stage. The strand-plain margin (Figure 1) marks both the innermost limit of the transgressive coastal barrier and the starting-line of the subsequent strand-plain progradation. The evolution of the delta plain is discussed in numerous papers, formerly mostly focused on morphology (Amenduni, 1884; Bocci, 1892; Chiesa and Gambarini, 1744; D'Arrigo,1932; Oberholtzer, 1875) and, more recently, on stratigraphic evidence (Bellotti et al., 1989, 1994, 1995; Belluomini et al., 1986; De Angelis d'Ossat, 1938; Dragone et al., 1967).

The Tiber river delta plain is of great archaeological interest because of the widespread, impressive and well-preserved ruins of Roman settlements (Figure 1). These include the town of Ostia, whose natural harbor was the first landing place of Rome, and the town of Portus with two artificial harbor basins named after emperors Claudius and Trajan, in AD 52 and 112, respectively. Altogether, including the facilities of the nearby town of Portus, the Ostia harbor was by far the main port in terms of size and trades in the Mediterranean Sea. In addition, the Portus necropolis, at the sides of Via Flavia-Via Severiana (the Roman coastal roads starting between the two Tiber river channels), the Vicus Augustanus village and the numerous luxury patrician *domus* built on the S delta reach (Laurentine shore) testify to the intensive exploitation of the area. Several accounts provide detailed data on the morphology and evolution of the deltaic area where the two Imperial port basins were excavated (Bellotti et al., 2009; Di Bella et al., 2007; Giraudi et al., 2009; Goiran et al., 2009a, b;

Keay et al., 2005) and the evolution of the Laurentine shore (Rendell et al., 2007). Conversely, Ostia and its surroundings still lack a comprehensive geologic framework, and the origin of Ostia and the main features of its harbor are still debated. According to historical sources (Livy, *Ab urbe condita* I, 33) Ostia was founded by king Ancus Marcius around 640 BC. However, the first archaeological evidence of the pristine *castrum* dates back to the fourth century BC. The Ostia harbor, located on the river channel according to the written sources, is witnessed only by remnants too scant and dismantled for a sound archaeologic framework.

Materials and methods

The present multidisciplinary study is based on the following materials and methods:

(a) Geomorphologic analysis from sets of aerial photographs (taken by Royal Air Force and Italian Aviation in 1943 and 1957, respectively) and the 2009 Digital Globe satellite imageries.

(b) Drilling of six cores (up to 4.5 m depth), located according to the investigations of De Angelis d'Ossat (1938), by means of an AF coring system produced by AFgtc s.r.l. (Ambrosio et al., 1999; Principe et al., 1997). Both equipment and technique were suitable for recovering continuous cores with preserved sedimentary structures.

(c) Grain size analysis of the collected sediments by means of mechanical sieving and laser diffractometry for > and < 62 μm fractions, respectively.

(d) ^{14}C datings, $^{13}C/^{12}C$ and C/N ratios, measured on specimens of the cored sediments selected according to the nature of the organic relics, stratigraphy and environmental implications. The ^{14}C readings were taken with the LSC (Liquid Scintillation Counting) technique except sample LTL4271A, whose modest weight required the AMS (Accelerator Mass Spectrometry) technique. Samples were preliminary mechanically and chemically processed to remove inorganic/organic contaminants: protocol details are reported elsewhere (Calderoni and Petrone, 1992). The C/N and $^{13}C/^{12}C$ ratios of the organic matter were measured by means of an elemental C and N analyzer and a Finnigan mass-spectrometer, respectively.

(e) Palaeontological analysis: 25 sediment samples were analysed from different depths from the six cores. Molluscs and foraminifers have been recorded. The specimens of the

species from each distinct mollusc assemblage have been counted. The adopted distinctive ecological character of each species (ecological classes) complies with the classical guidelines after Ložek (1964) for Quaternary non-marine molluscs. As for the non-marine taxa not reported by Ložek (1964), the ecological requirements for each species follow Kerney and Cameron (1979) and Giusti and Castagnolo (1982). The ecological attribution of brackish taxa is defined after Pérès and Picard (1964). The palaeoenvironmental reconstruction for the individual assemblages relies on the quantitative data of molluscs and the presence of foraminifers.

(f) Pollen analysis: 20 samples from core S5 were chemically treated with HCl (37%), HF (40%) and NaOH (10%). Pollen grains were identified according to Beug (2004), Reille (1992, 1995, 1998) and the reference collection at 'Sapienza' University (Rome). In average more than 300 terrestrial pollen grains/sample were counted. The pollen diagram was plotted using the computer program Psimpoll 4.25 (Bennett, 2005). The main percentage sum is based on terrestrial pollen, excluding pollen of hydrophytes, ferns and non-pollen palynomorphs (NPPs).

Results

Geomorphology

At Capo due Rami (Figure 1; *c*. 3 km inland) the Tiber river splits into two distributaries. The subordinate one (Fiumicino channel), flowing almost perpendicular to the coast, is the evolution of a Roman artificial channel (Fossa Traiana) dredged in the first-second century AD to connect the Imperial harbor to the Tiber river. The main distributary (Fiumara Grande) first parallels the coast over *c*. 1.5 km, then turns to WSW with a sharp elbow-shaped curve, and reaches the sea. Until September 1557, Fiumara Grande formed a wide meander *c*. 0.8 km landward before reverting seaward (M in Figure 1). Most of the Roman Ostia town spread on the Fiumara Grande left bank, close to the mouth of Tiber river in Roman times. According to Dionysius of Halicarnassus (*Romanae Antiquitates*, III, 44) in the first century BC the harbor provided landing facilities to vessels of up to 3000 *moggi* (some 9 tons of displacement), though confined in the Fiumara Grande channel. The meander bank was close to the edge of a coastal lake/marsh, known as Lacus Ostiae (Livy, A*b urbe condita* XXVII, 11, 2). Bertacchi (1960) argued that this coastal natural basin could have been used as an ancillary harbor . The marshy area, partly below the sea level, was fully reclaimed at the end of the nineteenth century (Amenduni, 1884).

Based on different approaches, the pre-Roman mouth of the Tiber river was considered to be located N of the present one, in the area now encompassing the Fiumicino channel and Capo due Rami (Giraudi, 2004; Giraudi et al., 2006, 2009; Goiran et al., 2007). This ancient river mouth, resulting from the evolution of the bay-head delta of 7000 BP (Bellotti et al., 2007), is revealed by the change of the beach ridge pattern from parallel to divergent, as pointed out by a magnetometric survey (Figure 2; Keay et al., 2005). Giraudi (2004) and Giraudi et al. (2006) argue that the pre-Roman river mouth prograded over some 2.5 km before being definitively abandoned at 760–410 cal. BC (Giraudi et al., 2009) or 790–370 cal. BC (Goiran et al., 2009b).

On the W rim of the ancient Ostia marsh, the aerial photographs show a 0.2 km wide belt of beach ridges, NW–SE oriented (α in Figure 3) along with a belt of WNW–ESE aligned ridges (β in Figure 3), stemming from the W limit of α. This latter (β) is recognizable from its origin up to near the left bank of the meander cut off in 1557, close to the Roman Ostia ruins. The insertion angle between the ridges of the two belts, some 10° for both the innermost and the outermost ones, rises to 30° for the intermediate ridges. The insertion of each ridge on the preceding one shifts away from the channel, in agreement with the 'c' and 'd' accreting patterns in the Arno river strand-plain (Kukavicic and Pranzini, 2003). Moving seaward, the beach ridges on which most of Roman Ostia is found are confined and cut by the single beach ridge γ (Figure 3), fairly conforming to the 'g' eroding pattern after Kukavicic and Pranzini (2003). The γ beach ridge marks a smoothed coastline stretching southward from Torre Boacciana (a military tower, recurrently restored up to AD 1420 and supposedly built on the Roman lighthouse) to Porta Marina (a passageway to the sea through the Ostia walls erected by dictator Lucius Cornelius Sulla Felix in 80 BC).

North of the Fiumara Grande meander abandoned in 1557, no beach ridges are found; however, the channel swinging, which produced the abandonment of the meander, has been tracked. On the right bank of the present channel the only relic of the ridge belt β is found as a feebly curved ridge intercepting the channel just upstream of Torre Boacciana. This shows a smooth flex close to the Fiumicino channel, where the most ancient cusp likely developed. Seaward, the N reach of the γ line appears as a weakly curved beach ridge almost paralleling the Imperial Portus-Ostia road. Finally, the most westward beach ridges belt (δ in Figure 3) pinpoints the post-Roman progradation at the mouths of the Fiumicino channel (excavated during the second century AD) and Fiumara Grande.

Stratigraphy

In addition to a thorough review of the stratigraphy of previous cores from the former Ostia marsh and its vicinity (De Angelis d'Ossat, 1938), new chronostratigraphic and palaeoenvironmental data are provided by six sediment cores (Figure 3). Cores S1 and S6 come from the most ancient beach ridges belt α, and the W rim of the marsh, respectively. Cores S2, S3, S4 and S5 were drilled in the former Ostia marsh. The stratigraphy and environmental reconstruction of the drilled sediments are summarized in Figure 4. Cores S1 and S6 display foreshore, backshore, dune and backdune sediments. A subfossil bone from the backshore sediments of S1 has been dated at 1890–1750 cal. BC (Table 1). sssA buried construction, revealed by brick, travertine and mortar fragments, constrained S6 core to a depth of 2.2 m; this core is located 100 m northward a buried wall uncovered in 1959 (Isaja and Lattanzi, 1992), recently excavated and tentatively referred to a pier remnant.

An almost clast-free peat level retrieved in cores S3 and S5 indicates a significant hiatus of marine and/or fluviatile input into the coastal lacustrine/marsh basin. A fluvial fill at the bottom of core S2, beneath brackish sediments, consists of thin muddy-sand sharp-based levels with some current ripple laminations, intercalated within dissected mud and calcretes including terrestrial mollusc fragments. Scant peat debris at *c*. 1 m depth in the S4 core were likely reworked and scattered within sediments of supposedly coastal marsh environment. The facies at the bottom of S4 is uncertain because of the absence of sedimentary structures and fossils.
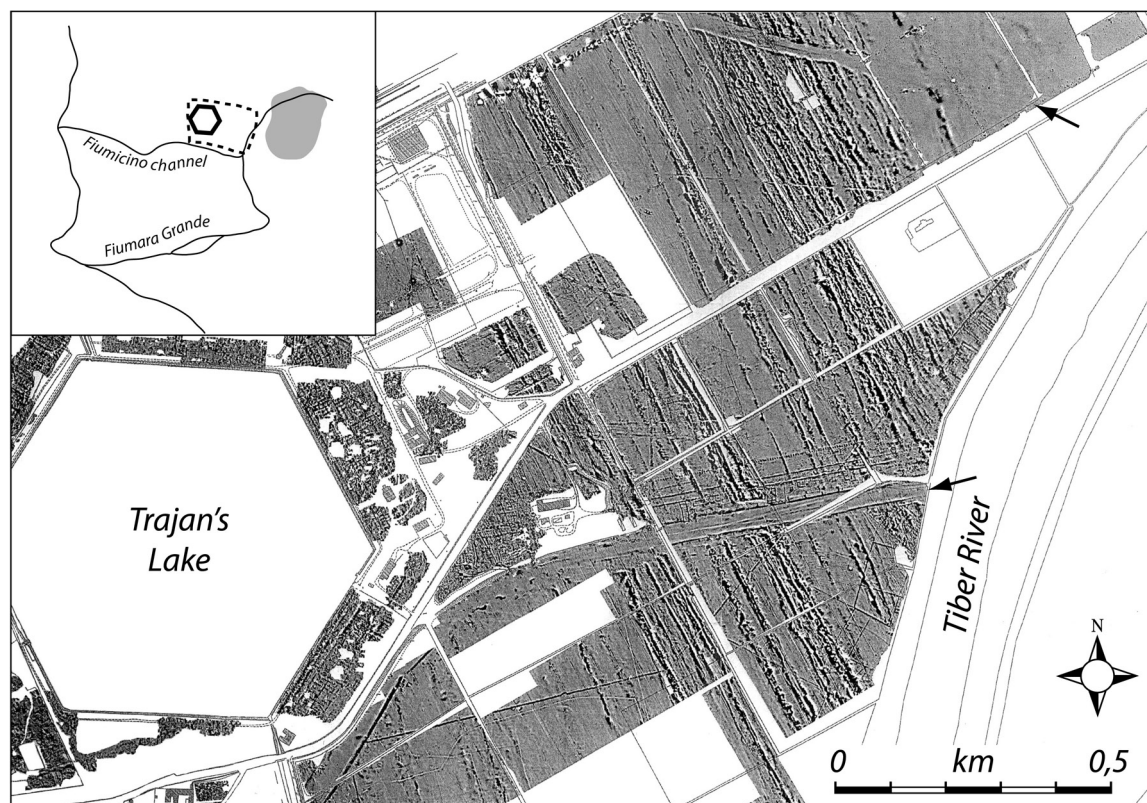
Figure 2. Magnetometric survey of the Capo due Rami area (modified from Keay et al., 2005) showing the oldest beach ridges to the right of the Tiber river. The ridges were cut by the artificial channels (arrows) dug during the construction of the Claudius and Trajan harbors (first and second centuries AD). The gray area on the upper left side shows the location of the bay-head delta around 7000 yr BP

14C readings, C/N and 13C/ 12C ratios

Table 1 shows the analytical results for the measured samples along with a few details on their origin and nature. In particular ^{14}C ages, calculated according to conventions and recommendations after Stuiver and Polach (1972), are reported at the $\pm$ 1σ level of uncertainty as yr BP and cal. BC. To point out at first glance the chronological relationships between natural events and the archaeological framework, both new and literature ^{14}C ages mentioned in the text are expressed as calibrated BC/AD intervals. The calibration software after Ramsey (2005) has been used throughout.

The investigated area experienced a complex evolution, reflected on the one hand by the stratigraphic array and on the other by the recurrent change in space and time of the represented sedimentation environments. In such a context the feasibility of ^{14}C chronology is heavily hampered by the availability of materials fully complying with the compulsory prerequisites of ^{14}C dating in terms of origin and nature. A previous study (Calderoni et al., 1997) reported several examples of biased ages yielded by organics scattered in a deltaic sedimentary suite due to the alternating organic matter inputs from terrestrial vegetation, marine sources and floating/submerged pondweeds living in the marshy and lagoonal environment. To insure against this risk we previously checked, by means of the ^{13}C/^{12}C and C/N ratios, whether the dated organic debris were derived from plant material formed through assimilation of tropospheric CO_2 and therefore suitable for dating.

Apart from a small bone fragment (sample LTL4271A, 1890–1750 cal. BC) the analyzed samples consisted of a fine-grained mineral matrix with abundant content of organic matter,

compacted and severely humified by diagenesis. In some samples the occurrence of macroscopic vegetal litter debris was not evident: their uniform black color, however, depended on the notable humic matter content, likely originated in situ from the break-down of the ancestor, and trapped by the clay and silt minerals. The organic matter survival, particularly for the less refractory fractions dispersed at macromolecular level, was favoured by acid pH values (because of the carboxylic groups of the first formed humic matter) coupled with reducing conditions (because the fine grained sediments were an effective barrier against oxygen penetration). The C/N ratio dated organic matter ranges from 16.0 (Rome-2066) to 12.8 (Rome-2068), thus matching the values reported for organic relicts resulting from break down of subaerial plant biomass (Prahl et al., 1980). The variability exhibited by the C/N ratios is accounted for by the different decomposition pathways, locally experienced by the vegetal debris, which removed selectively the constituents of the primitive organic matter input. The C/N ratios suggest that the dated organic matter reasonably derives from only one source, in particular from subaerial vegetation. The δ^{13}C values, ranging from −26.0 (‰) (Rome-2066) to −23.4 (‰) (Rome-2070), are typical of terrestrial vegetation remnants (C3 pathway cycle), subjected to a mild early diagenesis causing only a slight ^{13}C enrichment due to the customary selective removal of the ^{12}C-enriched constituents. Thus, the δ^{13}C values are consistent with the C/N ratios in suggesting a parental subaerial vegetation for the dated organic matter. Further, the δ^{13}C values for the sample pairs Rome-2066/-2067 and Rome-2069/-2070 are of some concern, as in both cases a clear trend of ^{13}C rising with depth is noticeable. As the C isotope composition of organic matter during the first diagenesis turns heavier with time, the observed trend rules out any reworking of the cored sequence,
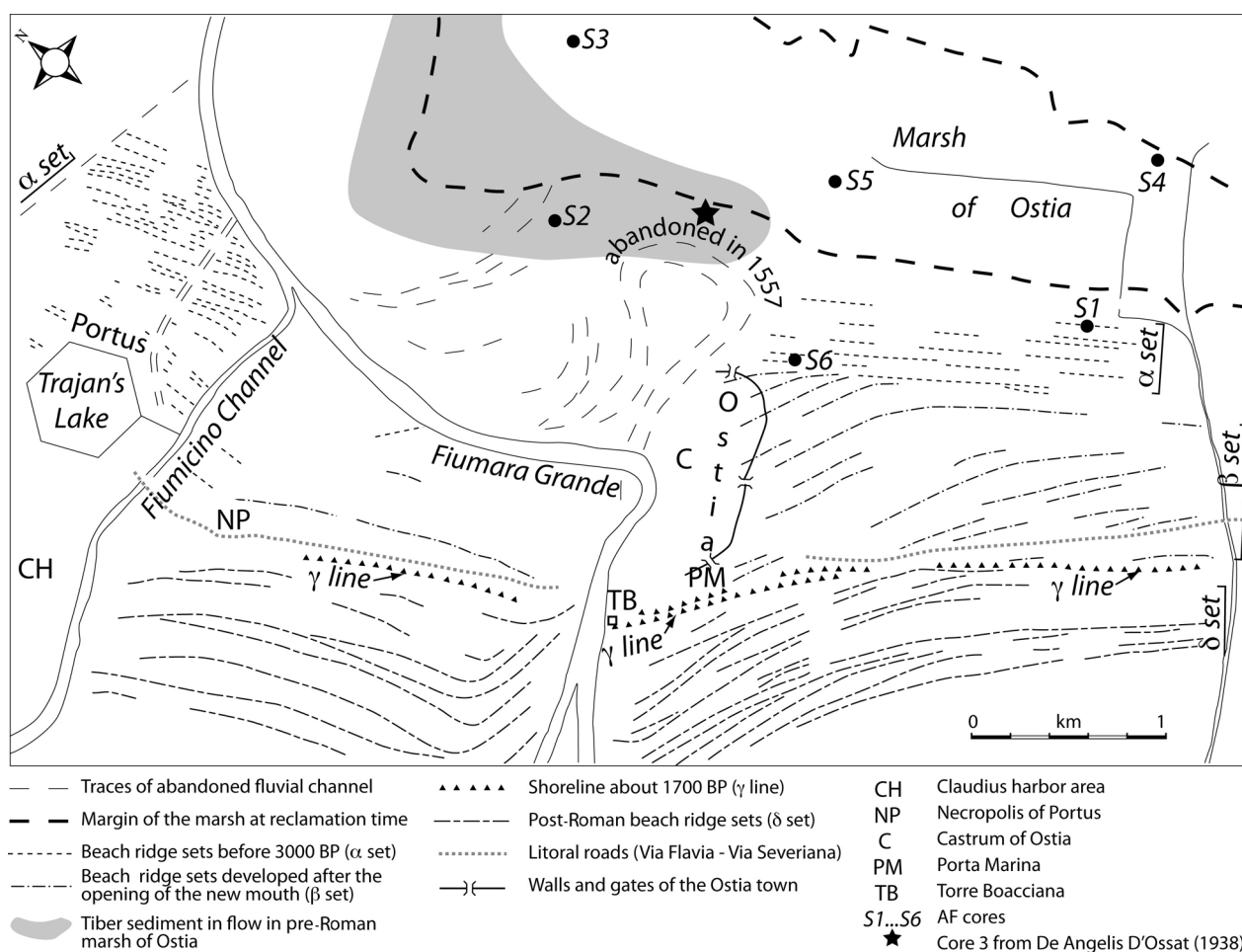
Figure 3. Morphological features of the delta plain gained by analyzing aerial photographs

therefore strengthening reliability and significance of the ^{14}C readings. Including the bone sample LTL4721A, ^{14}C readings cluster at c. 900–540 cal. BC and c. 1900–1200 cal. BC, thus spanning the last 3500 years. For cores S3 and S5, which provided two organic matter layers at distinct depths, a fair chronostratigraphic coherence is evident: in core S3 the ^{14}C readings were 2720±50 (Rome-2066, 2.0 m) and 3465±55 BP (Rome-2067, 3.1 m) and in core S5 2555±50 (Rome-2069, 3.0 m) and 3375±55 BP (Rome-2070, 4.2 m), respectively. The different depths where synchronous organic matter deposits occur depend upon the variable palaeosurface of the marsh bottom and the effects of the compaction process. Thus, the four datings suggest that the marsh witnessed two low-energy phases, separated by some 700/800 years, suitable for the development of a freshwater aquatic environment. The two ^{14}C readings for core S4, Rome-2068 and Rome -2071, are relative to the same level, 1.1 m deep, which contained organic matter distributed in macro aggregates as nodules and/or discontinuous thin layers. This level was dated in duplicate because the poor organics content in the first sample (Rome-2071) gave rise to a reading (3170 BP) affected by 100 years of uncertainty. Sediment from a very close core yielded, at the same depth, a more adequate amount of material, dated (Rome-2068) at 3040±55 BP. By considering the uncertainties, the two ages are undistinguishable at ± 1σ level and therefore their weighted mean (3070±50 BP) has been considered. Owing to its discontinuous distribution, the origin of the organic matter in this level is puzzling, as it can be referred either to scattered primary small accumulation spots

or to a secondary deposition. For this reason, we do not rely on the age of this level to implement the overall framework of the study area.

Faunas

Widespread mollusc assemblages and frequent foraminifers were found in the collected sediments. Bottom to top, the identified faunal assemblages are as follows (Table 2):

(1) Core S1. At −2.30 m, few reworked fragmentary decalcified hinges of marine or brackish bivalves (*Abra* sp., Cardiidae indet.) occur. Scarce terrestrial molluscs, mainly represented by the gastropods *Theba pisana* and *Cochlicella barbara*, characteristic of a backdune environment (Giusti and Castagnolo, 1982), are present in the sandy sediments of the upper part of the core.

(2) Core S2. From −3.20 to −2.15 m the muddy sediment yielded only fragments of terrestrial molluscs. At −1.85 m scarce and reworked marine littoral foraminifers, such as *Ammonia tepida, Elphidium crispum* and *Lobatula lobatula*, and one shell of terrestrial Hygromiidae are present. At −1.40 m, in muddy-sandy sediment, a rich assemblage of brackish gastropods and bivalves, such as *Hydrobia ventrosa*, *Abra segmentum* and *Cerastoderma glaucum*, accompanied by brackish foraminifers, such as *Ammonia parkinsoniana* and *Haynesina germanica*, point to a brackish shallow water environment.
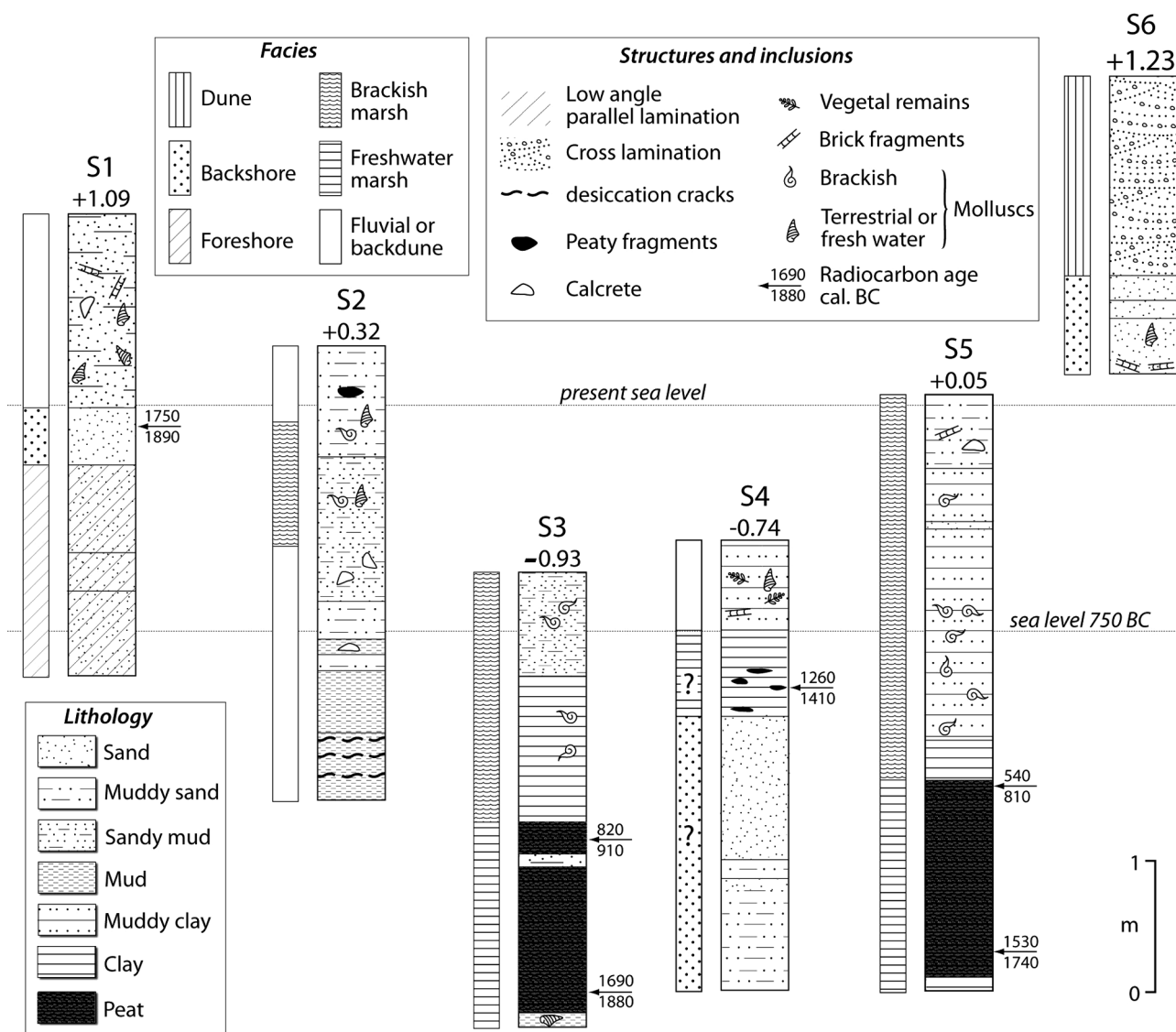
Figure 4. Drilling logs and environmental interpretation. Elevation of the drilling points in meters. Sea levels at 750 BC (after Lambeck et al., 2004) and present times are also shown

The terrestrial molluscs, *Vitrea subrimata* and Hygromiidae indet. mixed up with freshwater taxa, such as *Gyraulus* sp. and opercula of *Bithynia* indicate the vicinity of an emerged environment. At −0.35 m, frequent terrestrial molluscs, such as *Cernuella virgata* typical of dry, exposed sites/dunes near

the sea (Kerney and Cameron, 1979), occur together with plant remains pointing to a backdune environment.

(3) Core S3. The muddy sediments at −3.35 m contain a rich freshwater mollusc assemblage dominated by *Bithynia* species. *Armiger crista,* a freshwater gastropod, and *Oxyloma elegans,*

Table 1. Radiocarbon ages measured on the organic matter isolated from the studied sediment cores

Sample identifier	Core # (depth in core, m)	Material	Conventional ^{14}C age (yr BP)	Calibrated age[a] (cal. BC)	$\delta^{13}C$[b] (‰, vs. SMOW)	C/N
LTL4271A	S1 (1.6 m)	bone fragment	3520 ± 40	1890–1750	−21.7	
Rome-2066	S3 185 (2.0)	peat level	2720 ± 50	910–820	−26.0	16.0
Rome-2067	S3-250 (3.1)	peat level	3465 ± 55	1880–1690	−24.8	15.4
Rome-2068	S4-070 (1.1)	peat debris	3040 ± 55	1390–1210	−23.1	12.8
Rome-2071	S4-070 (1.1)	peat debris	3170 ± 100	1600–1260	−23.7	13.4
Weighted mean for Rome-2068/-2071			3070 ± 50	1410–1260	mean: 23.4	mean: 13.1
Rome-2069	S5-250 (3.0)	peat level	2555 ± 50	810–540	−25.0	15.6
Rome-2070	S5-320 (4.2)	peat level	3375 ± 55	1740–1530	−23.4	14.7

[a]Calibration performed with the software after Ramsey (2005).
[b]Uncertainty ranges from ± 0.25 to ± 0.15 permill.

Table 2. Absolute abundance of molluscs in the analyzed six cores. Legend: EC, ecological classes (after Ložek, 1964); IW, wood species; 4S, species of dry/sunny areas devoid of arboreal vegetation; 7M, mesophilous species of damp or dry areas; 9P, strongly hygrophilous species of marshes or similar very damp to wet areas; IOS, IOSF, aquatic species of still waters and/or flowing waters; IOP and IOPp, aquatic species of marshes and shallow waters rich in vegetation and/or ephemeral marshes; IOS(F), aquatic species of still or, subordinately, flowing waters; LEE, lagonal Eurythermal and Euryhaline biocoenosis (after Pérès and Picard, 1964); ap, apexes; fg, fragments; a, abundant; r, rare; *, number of the most represented right or left valves; X, foraminifer occurrence; R, reworked

MOLLUSCS	EC	Core Sample																						
		S1				S2						S3			S4				S5				S6	
		−0.60	−0.80	−1.20	−2.30	−0.35	−1.40	−1.85	−2.15	−2.50	−3.20	−1.00	−1.20	−3.35	−0.35	−1.45	−2.45	−2.75	−0.74	−2.10	−2.70	−2.89	−1.40	−1.60
Terrestrial																								
Oxyloma elegans (Risso)	9P													8										
Limax sp.	7M														2									
Vitrea subrimata (Reinhardt)	IW						1																	
Cecilioides acicula (O.F. Müller)	4S									fg													1	
Cernuella virgata (Da Costa)	4S					1									2									
Cochlicella virgata (Linné)	4S	1	4			27	10								9				1				fg	
Theba pisana (O.F. Müller)	4S		10																					
Hygromiidae									2	1														
Helicidae																fg								
Freshwater																								
Physa cfr. fontinalis (Linné)	IOS																							
Lymnaea peregra (O.F. Müller)	IOS(F)												2		2									
Anisus spirorbis (Linné)	IOPp														13									
Armiger crista (Linné)	IOS											1				1								
Gyraulus sp.	IO								2			2			3									
Valvata cristata O.F. Müller	IOP											9												
Bithynia leachi (Sheppard)	IOP												28											
Bithynia tentaculata (Linné)	IOSF												30											
Bithynia sp.	IO												549ap			a					1ap			
Bithynia opercula	IO									r		r				a			r					
Sphaerium cfr. corneum (Linné)	IOS(F)											1												
Brackish water																								
Hydrobia ventrosa (Montagu)	LEE					241						>1000							>1000	>1000	>1000			
Abra segmentum (Récluz)*	LEE					31						23	8						64	68	390	77		
Cerastoderma glaucum (Récluz)*	LEE					39						15	16		1				158	179	434	43		
BENTHIC FORAMINIFERS																								
Ammonia parkinsoniana (d'Orbigny)						X						X							X	X	X			
Ammonia tepida (Cushman)								X	X			X	X						X	X				
Elphidium crispum (Linné)																								
Elphidium paucilocullum (Cushman)								X					X						X		X			
Haynesina germanica (Ehrenberg)							X						X								X			
Lobatula lobatula (Walker & Jacob)								X																
Foraminifera indet.										R								R						R

hygrophilous species living in marshes or comparably very damp or wet places, are the accompanying taxa: as a whole the fauna suggests palustrine-lacustrine conditions. At −1.20 and −1.00 m rich brackish water assemblages dominated by *H. ventrosa, A. segmentum, C. glaucum*, and foraminifers, such as *A. parkinsoniana, A. tepida, Elphidium pauciloculum* and *H. germanica*, occur. Several freshwater molluscs typical of slowly flowing or standstill water, such as *Physa* cfr. *fontinalis* at −1.20 m depth, and *Lymnaea peregra, Valvata cristata, Armiger crista* and *Sphaerium* cfr. *corneum* at −1.00 m, point to a freshwater input in the lagoonal environment.

(4) Core S4. At −2.75, −2.45 and −1.45 m (lower and intermediate core portions) fossil-free sandy sediments were found. At −0.35 m terrestrial gastropods, such as *C. virgata* and *Limax* sp., and freshwater taxa, such as *Anisus spirorbis, Gyraulus* sp. and *Lymnaea peregra*, account for an emerged environment with scattered small pools with standstill or slowly flowing water.

(5) Core S5. At −4.40 and −3.44 m the peat level is devoid of fossils. In both middle (−2.89, −2.70 m) and upper (−2.10 and −0.74 m) core portions, brackish mollusc and foraminifer assemblages were detected. The former, dominated (>1000 specimens/sample) by *H. ventrosa*, also includes abundant *C. glaucum* and *A. segmentum*. The abundant foraminifers are represented by *A. parkinsoniana, A. tepida* and *E. pauciloculum*. A lagoon environment is inferred.

(6) Core S6. This mostly sandy core only provided scarce mollusc fauna. Apart from scattered plant debris, very scant and fragmented terrestrial molluscs, such as *Hygromiidae* indet. and *Cecilioides acicula*, were observed at −1.60 and −1.40 m depth. An emerged environment is inferred throughout.

Palynology

The results of pollen analysis (core S5) are presented as a percentage diagram in Figure 5. Selected taxa of the following ecological groups are displayed: conifers, riparian trees, deciduous trees, evergreen trees and shrubs, anthropic indicators, herbaceous taxa, hydrophytes, ferns, and NPPs. Pollen was generally well preserved, with less than 8% of indeterminable grains. The pollen record reveals a high floristic richness: 98 taxa have been identified, including pollen, spores and other palynomorphs. The pollen diagram highlights the vegetation history from *c*. 1900 BC to AD 600.

Between 1900 and 600 BC (pollen zone Ost S5-a) the marshland S of the Tiber delta was characterized by sedge vegetation. The presence of Nymphaeaceae, Lythraceae, *Callitriche* and *Myriophyllum* points to a freshwater pond. Around 1100 BC there is evidence of a possible temporary drying of the marsh, colonized by pioneer taxa, as suggested by peaks of Asteroideae, Apiaceae and ferns. This hypothesis is supported by high values of *Pseudoschizaea* and *Glomus*, indicating temporary desiccations with erosional processes in the basin (Pantaleón-Cano et al., 2003; Scott, 1992; van Geel, 1986). Regionally, between 1900 and 600 BC the landscape was covered by a mixed oak-dominated woodland with evergreen elements. Locally, as a consequence of the accretion of the delta cusp, after *c*. 1000 BC there is a spread of arboreal vegetation, especially evergreen and deciduous *Quercus* and *Juniperus*, suggesting the expansion of forest communities on the newly available land. Indicators of human activity are

scanty, probably because of environmental instability and/or unhealthiness of the marshy area.

Around 600 BC (pollen zone Ost S5-b), in correspondence with a lithological change from peat to clayey sediments, a hydrological change is recorded, involving the vegetation of both local aquatic domain and surrounding landscape. A sharp peak of foraminiferal lining (Figure 5), absent in the underlying pollen zone, points to a sudden intrusion of sea water into the basin (Limaye et al., 2007). As a consequence, a saline/brackish environment developed, also documented by the definitive disappearance of freshwater hydrophytes, an increase of Chenopodiaceae, and the appearance of *Ruppia*. Around 450 BC, a significant amount of cultivated and anthropochore plants is recorded, including a clear increase of *Olea, Vitis*, and Cannabaceae, along with a progressive appearance of cereals, *Mercurialis, Juglans*, and *Castanea*. The appareance of *Pinus pinaster/pinea* type suggests the introduction of cultivated pines by Romans. Comparable increases of *Pinus pinaster/pinea* have been also reported from several other sites of the central Mediterranean regions since the first century BC (Di Rita et al., 2010).

From 600 BC to AD 600 (pollen zone Ost S5-b), the arboreal vegetation was characterized by deciduous and evergreen oak-dominated forests. Mixed deciduous woodlands represented the main regional vegetation type inland (Magri and Sadori, 1999; Mercuri et al., 2002). Deciduous oaks also formed widespread planitial forests along the Tyrrhenian coast of the Lazio region (Di Rita et al., 2010), as it is still testified by modern remnants of natural vegetation in protected areas (Lucchese, 1996; Manes et al., 1997). The evergreen vegetation, well represented in the pollen diagram though progressively declining, was mainly distributed seaward and likely formed coastal 'macchia' woodlands and patchy communities within the mixed planitial forest.

Since the first century AD, a further dramatic increase of chenopods, peaking atop the sequence, is consistent with the development of saltworks, historically documented at Ostia during Imperial times. This trend is almost synchronous with an important increase of chenopods in the S portion of the Maccarese pond, located just N of the Tiber river delta (Di Rita et al., 2010), confirming the extensive exploitation of the large saltworks known as Campus Salinarum Romanarum (Lanciani, 1888). The increase of Cichorioideae and Chenopodiaceae detected atop the core sediments may be partly ascribed to selective pollen preservation due to sediment erosion processes, as indicated by a parallel increase of *Glomus*.

Discussion

According to the geomorphologic analysis, α is the most ancient ridge belt (Figure 3). It originated during the first episodes of the strand-plain formation, due to the conspicuous infilling of the former estuary basin because of the progressive deposition of the river solid load seaward. According to Giraudi (2004), the most ancient ridges (α belt), both N and S of the Tiber river, date back to 5700–6000 BP. Bellotti et al. (2007) argued that the transgressive coastal barrier stopped migrating inland around 7000 BP. When the Tiber river started discharging directly into the sea, the ancient estuary basin was split into two coastal lakes.

The northern basin (Maccarese pond), poorly communicating with the sea since around 5500 BP, has been the subject of many studies (Bellotti et al., 1995, 2007; Belluomini et al., 1986;
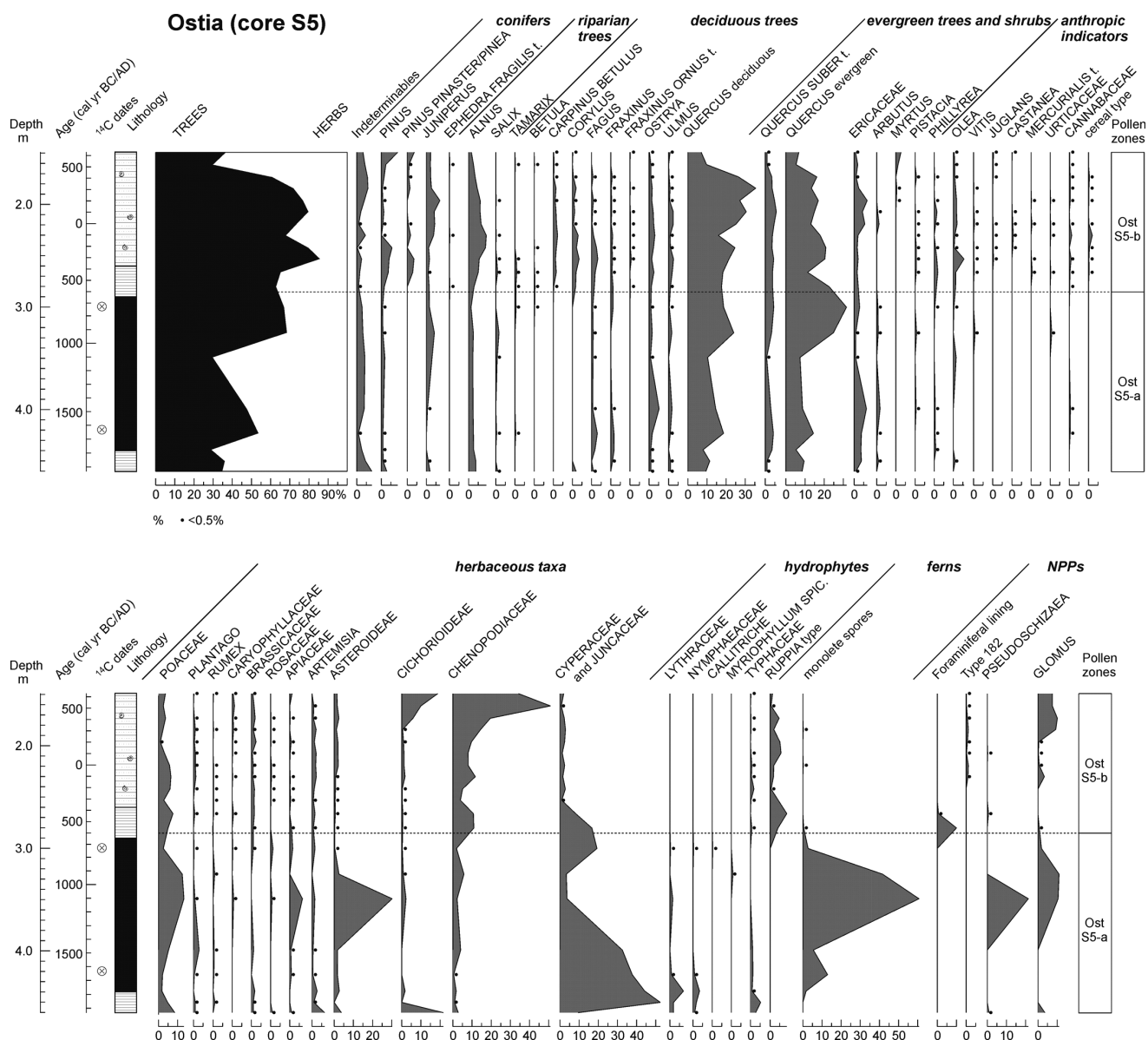
Figure 5. Pollen percentage diagram for core S5. The age–depth model was calculated by linear interpolation of ^{14}C readings

Carboni et al., 1998; Di Rita et al., 2010; Giraudi, 2002, 2004; Giraudi et al., 2006). By contrast, satisfactory data on the origin and evolution of the southern basin (Ostia marsh) are lacking. Our new evidence provides an *ante quem terminus* of some 4000 BP for its full development.

The slowly accreted delta cusp N of the present Fiumicino channel (α in Figure 3) formed following the progradation of a distributary mouth lying on the prolongation of a buried fluvial deposit (Bellotti et al., 2007). The appearance of this feature, likely under accretion around 3000 BC, pinpoints the embryonic phase of the wave-dominated Tiber river delta. Giraudi (2004) reported a delta cusp in this area and suggested that its dismantled relics could have been part of the seaward protection of Claudius harbor (Giraudi et al., 2006, 2009).

The migration of the Tiber river channel forming the first cusp was over at 760–410 cal. BC (Giraudi et al., 2009) or at 790–370 cal. BC (Goiran et al., 2009b). Before migrating, the Tiber river did not flood into the Ostia marsh, as indicated by the continuous peat level in cores S3 and S5, dated between 1880 and 540 cal. BC. A rough estimation of the peat deposition rate, based

on level thickness and ^{14}C readings, is 1.40 mm/yr. The overall stratigraphy of cores S2 and S3 (located in the northernmost part of the marsh) suggests that peat levels underly fluvial sediments. A sharp contact between peat and fluvial sediments is reported by De Angelis d'Ossat (1938) in his core 3. This sudden change of sedimentation pattern was possibly produced by a disruption of the left bank of the distributary. The consequent input of river water into the Ostia marsh implied solid load aggradation into its N reach (Figure 3). If so, the age 810–540 cal. BC (top of the peat level in core S5) may reasonably represent the beginning of the Tiber river discharge into the marsh, in agreement with the ages 760–410 and 790–370 cal. BC suggested by Giraudi et al. (2009) and Goiran et al. (2009b), respectively.

The Tiber river inflow rapidly raised the water level in the marsh (cf. the increase of *Alnus*, Figure 5), producing a new outlet through the sandy ridge belt, reaching the sea *c*. 2 km southeast of the previous river mouth (Figure 3). A sudden input of marine water into the basin is indicated by a peak of foraminiferal lining and the appearance of *Ruppia* at the basis of the clastic sediments in core S5 (Figure 5). A brackish environment is confirmed in
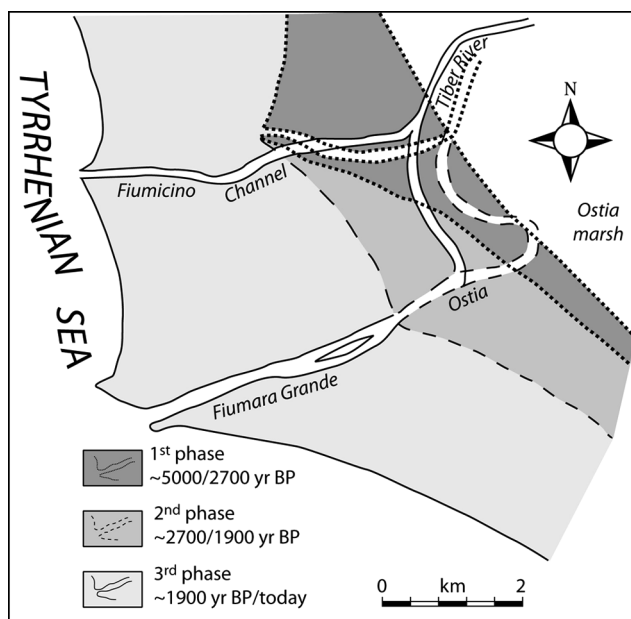
Figure 6. Main changes of the Tiber river mouth location during the strand-plain evolution

cores S2, S3 and S5 by the mollusc record. Assuming for the top of S5 the age AD 1890, corresponding to the beginning of the reclamation, the clastic sedimentation rate after the peat deposition can be roughly estimated 1.25 mm/yr. At the mouth of the new outlet a cusp formed, while the old one, no longer fed, underwent erosion. The river channel migration caused the new cusp to develop through a progressive cannibalization of the beach ridges on its right wing. The beach ridges accretion pattern reflects the fast growth of the new cusp, which was almost fully developed in the fourth century BC, as indicated by the location of the Ostia *castrum* on its left wing (Figure 3). The mouth progradation rate has been estimated 6 m/yr, a value not very dissimilar from the 9 m/yr measured at Fiumara Grande in the 1569–1744 timespan (Bersani and Moretti, 2008). This fast progradation rate likely gave origin to a cusp with elongated apex, a feature consistent with the historical account of Dionysius of Halicarnassus (first century BC), who defined the Tiber river banks as 'very seaward projected'. The dropping of the insertion angle shown by the most recent ridges of the cusp (β belt) reveals a decline of their growth rate, implying the erosion of the apex, as suggested by both the erosion pattern of the beach ridges and the smoothly curved shoreline (γ line). According to historical sources, this erosive process was underway in the third century AD. Minucius Felix (*Octavius* II, 3-4; III, 2-5; IV, 5) claimed that the almost straight shoreline in front of Porta Marina was protected by a stony barrier and an AD 238 epigraph mentions stone blocks arranged as a protection of the seaward side of Via Severiana southward the Tiber river mouth (Lanciani, 1903). Further, Cassius Dio (*Hist. Rom.* 60, 11, 1 ss) chronicled that 'close to the mouth the Tiber river banks did not provide enough protection for the vessels any more', thus hinting that the harbor potentialities, besides being inadequate for the huge trades of the Roman Empire, were also constrained by ongoing adverse environmental conditions.

After the Roman times, progradation (δ ridge belt) re-started at the mouths of Fiumara Grande and, discontinuously, of the Fiumicino channel (Figure 6). The last progradation cycle (from the Renaissance to the nineteenth century, Figure 6) progressively

hampered the functionality of the Imperial harbor, which was progressively isolated from the sea and definitively abandoned.

Although the above-mentioned environmental changes were strictly controlled by the local morphogenesis, they did also reflect global rapid climatic changes (RCC) events. In fact, the timing of the southward migration of the Tiber river mouth fits the 1550–550 cal. BC cooling phase (Mayewski et al., 2004) which corresponds to a humid phase (Lirer et al., 2009) for the Eastern Tyrrhenian margin. The increased river discharge on the one hand triggered the river channel instability and on the other hand sped up the progradation of the new cusp, so that the estimated progradation rate (6 m/yr) agrees with other records of the 'Little Ice Age' (LIA) (Bersani and Moretti, 2008). The erosion phase corresponding to the γ line reveals a warm climate episode before the first post-Roman progradation and almost contemporary to the cold/humid RCC event backdated at 750–950 cal. AD (Mayewski et al., 2004).

Far more intriguing is to asses the role of human activity in the dynamics of the environmental changes over the seventh to fifth centuries BC, that is during the early development of Ostia. Around 600 BC, a sudden sea water intrusion appears to be the main factor turning the freshwater body into a saltmarsh. It is difficult to ascertain whether this event was caused by an entirely natural opening of the sandy barrier towards the sea, or it was also influenced by a deliberate human action. The latter hypothesis is consistent with written sources, indicating that Ostia was founded in 640 BC to control the local saltworks. In the Maccarese pond north of the Tiber delta, well documented Etruscan saltworks of the sixth century BC (Morelli et al., 2004) are recorded by a modest increase of chenopods (Di Rita et al., 2010). The coeval increase of chenopods in the Ostia S5 record, complemented by the appearance of *Ruppia*, is much more evident and supports the hypothesis that the Romans may have taken advantage of a sudden sea water intrusion event to set the Ostia saltworks. This conclusion highlights also the possibility that around 600 BC the disruption of the narrow sandy barrier may have been favoured and successively managed by the Romans, with the aim of converting the area in saltworks. Though trivial, we recall that the Romans lacked neither cheap manpower nor hydraulic engineering knowledge. However, archaeological data point out that the Ostia settlement spread and gained importance only in the fourth century, more or less contemporarily with the significant appearance of cultivated and anthropochore plants in the pollen diagram.

Conclusions

The Tiber river delta strand-plain developed through three main river migration steps recorded by the distinct position of the correspondent beach ridge deltaic cusp. In the first step, from *c*. 3000 BC to the eighth to seventh centuries BC, a cusp developed over the area stretching from the present Capo due Rami to the site where the Imperial harbor was subsequently built. Both the cusp and the coeval rectilinear beach-ridges rimming the Ostia marsh are suggestive of an arcuate shoreline of the embryonal wave-dominated delta. The transition to the next stage is marked by an abrupt Tiber river discharge into the Ostia marsh. The marsh flooding is pointed out by the landward shift of the fluvial channel which originated the Fiumara Grande meander. After the opening of the Fiumicino channel (early second century AD) the delta progradation resulted in a complex cusp system built up by the two distributaries almost simultaneously active (third evolution phase). The progradation is still ongoing, having particularly intensified

over the last 500 years. The timing of the main strand-plain evolution phases possibly matches some global rapid climatic changes. In particular, cold/humid periods affected the mouth stability (causing avulsions and/or progradation) and, conversely, warm/dry phases eroded the deltaic beach.

The vegetation of Tiber delta experienced major changes, involving both terrestrial and aquatic environment, in response to the progression of the deltaic cusp and of the shifts of the Tiber distributary. Between 1900 and 600 BC the landscape was covered by a mixed oak-dominated woodland with evergreen elements. The marshland S of the Tiber delta was characterized by sedge vegetation in a freshwater environment. Around 600 BC, the sudden intrusion of sea water into the basin induced a saline/brackish environment and changed the marshland into a chenopod-dominated saltmarsh with widgeon grass meadows. From 450 BC onwards, a significant amount of cultivated and anthropochore plants indicates an intensive exploitation of the area by human communities. High frequencies of chenopods suggest the existence of local saltworks, which had a considerable development in Imperial times (first century BC).

Our results clarify the apparent discrepancy between historical sources and archaeological evidence, which set the origin of Ostia around 640 BC and the fourth century BC, respectively. Around 640 BC, the Tiber river mouth had just migrated, and the new cusp had not yet formed (early second phase). Thus, the beach-barrier separating the Ostia marsh from the sea was still too narrow and unsafe against storms and/or river mouth migrations for permanent human occupation. Further, even the immediately inland area, mostly marshy and crossed by a migrating river channel, could hardly provide adequate settlement locations. Therefore, in the seventh century BC there could be only an outpost with the purpose of controlling the strategic river mouth and, possibly, setting up salt extraction from the marsh. In fact, starting from approximately 600 BC both pollen and mollusc data indicate that the marsh turned into a brackish environment. Only subsequently, around 450 BC, when the cusp extended more than 1 km seaward, the available sandy land was wide and safe enough to set a fortified camp (*castrum*) and develop saltworks. Brick, travertine and mortar fragments at the bottom of core S6 from the edge of the Ostia marsh suggest the presence of permanent buildings, likely belonging to peripheral infrastructures of the harbor.

The geomorphologic, sedimentologic and palynological data from the ancient marsh of Ostia highlight complex sea–lake–man interactions. While the natural progradation of the delta cusp was the main factor determining the land availability for the construction of the town of Ostia, it cannot be excluded that the Romans could have so intensively managed this territory since 600 BC onward to modify its physiography. In fact, they probably established the saltworks in the Ostia marsh managing, and possibly causing, the disruption of the sandy barrier between the Ostia marsh and the Tyrrhenian Sea.

Acknowledgements

References

Ambrosio M, Dello Monaco G, Fagioli MT, Giannini F, Pareschi MT, Pignatelli L et al. (1999) Utilizzo di fioretto meccanico e carotiere microstratigrafico inguainante per la valutazione degli spessori e della stratigrafia delle coltri vulcanoclastiche soggette a fenomeni di colata rapida di fango. *Geologia Tecnica & Ambientale* 4: 23–32.

Amenduni G (1884) *Sulle opere di bonificazioni della plaga litoranea dell'Agro Romano che comprende le paludi e gli stagni di Ostia, Porto, Maccarese e delle terre vallive di Stracciacappa, Baccano, Pantano e Lago dei Tartari*. Roma: Eredi Botta.

Arnaud-Fassetta G and Provansal M (1999) High frequency variations of water flux and sediment discharge during the Little Ice Age (1586–1725 AD) in the Rhône Delta (Mediterranean France). Relationship to the catchment basin. *Hydrobiologia* 410: 241–250.

Arnaud-Fassetta G, Carre MB, Marocco R, Maselli Scotti F, Pugliese N, Zaccaria C et al. (2003) The site of Aquileia (northeastern Italy): Example of fluvial geoarchaeology in a Mediterranean deltaic plain. *Geomorphologie* 4: 227–246.

Bellotti P, Calderoni G, Carboni MG, Di Bella L, Tortora P, Valeri P et al. (2007) Late Quaternary landscape evolution of the Tiber River delta plain (Central Italy): New evidence from pollen data, biostratigraphy and ¹⁴C dating. *Zeitschrift für Geomprphologie* 51(4): 505–534.

Bellotti P, Carboni MG, Milli S, Tortora P and Valeri P (1989) La piana deltizia del Fiume Tevere: Analisi di facies ed ipotesi evolutiva dall'ultimo 'low stand' glaciale all'attuale. *Giornale di Geologia* 51(1): 71–91.

Bellotti P, Chiocci FL, Milli S, Tortora P and Valeri P (1994) Sequence stratigraphy and depositional setting of the Tiber delta: Integration of high resolution seismics, well logs and archaeological data. *Journal of Sedimentary Petrology* B64: 416–432.

Bellotti P, Mattei M, Tortora P and Valeri P (2009) Geoarchaeological investigations in the area of the imperial harbours of Rome. *Méditerranée* 112: 51–58.

Bellotti P, Milli S, Tortora P and Valeri P (1995) Physical stratigraphy and sedimentology of the late Pleistocene–Holocene Tiber Delta depositional sequence. *Sedimentology* 42: 617–634.

Belluomini G, Iuzzolini P, Manfra L, Mortari R and Zalaffi M (1986) Evoluzione recente del Delta del Tevere. *Geologica Romana* 25: 213–234.

Bennett KD (2005) Documentation for Psimpoll 4.25 and Pscomb 1.03. C programs for plotting pollen diagrams and analyzing pollen data. Retrieved from http://chrono.qub.ac.uk/psimpoll/psimpoll.html (1 April 2010).

Bersani P and Moretti D (2008) Evoluzione storica della linea di costa in prossimità della foce del Tevere. *L'acqua* 5: 77–88.

Bertacchi L (1960) Elementi per una revisione della topografia ostiense. *Rendiconti Accademia dei Lincei* 8: 8–32.

Beug HJ (2004) *Leitfaden der Pollenbestimmung für Mitteleuropa und angrenzende Gebiete*. München: Verlag.

Blackmann DJ (2005) Archaeological evidence for sea level changes. *Zeitschrift für Geomorphologie* 137: 61–70.

Bocci D (1892) Il delta tiberino. *Giornale del Genio Civile* 30: 1–34.

Calderoni G and Petrone V (1992) Department of Earth Sciences at the University of Roma radiocarbon dates I. *Radiocarbon* 34(1): 105–113.

Calderoni G, Lombardo M, Turi B and Trudu C (1997) Geochemical evidences for biased radiocarbon ages yielded by multisource organic matter scattered in sediments. *Science and Technology for Cultural Heritage* 6(2): 175–183.

Carboni G, Conati Barbaro C and Manfredini A (1998) The Copper Age settlement Le Cerquete-Fianello (Maccarese, Rome) a sedentary community in the lagoon environment of Maccarese (Rome). In: Union Internationale de Sciences Préhistoriques et Protohistoriques (ed.) *Atti del XII Congresso* (Forlì, 8–14 settembre 1996), Abaco, 27–34.

Chiesa A and Gambarini B (1744) *Delle cagioni e de' rimedi delle inondazioni del Tevere. Della somma difficoltà di introdurre una felice e stabile navigazione da Ponte nuovo sotto Perugia fino alla foce della Nera nel Tevere, e del modo di renderlo navigabile dentro Roma*. Roma: Antonio De Rossi.

D'Arrigo A (1932) Sulle fasi di regime del litorale deltizio del Tevere. *Annali LL.PP* 70: 207–242.

Dalrymple RW, Zaitlin BA and Boyd R (1992) Estuarine facies models; conceptual basis and stratigraphic implications. *Journal of Sedimentary Petrology* 62: 1130–1146.

De Angelis d'Ossat G (1938) Geo-pedogenesi delle terre sul delta del Tevere. *Récherches sur le Sol* 6(2): 138–168.

Di Bella L, Bergamin L, Frezza V, Bellotti P and Carboni MG (2007) Paleoenvironments in the Roman Claudius Harbour at the Tiber River Mouth (Central Italy). Evidences from benthic foraminifera. In: European Geosciences Union (ed.) *IV General Conference 2007*. Copernicus GmbH.

Di Rita F, Celant A and Magri D (2010) Holocene environmental instability in the wetland north of the Tiber delta (Rome, Italy): Sea–lake–man interactions. *Journal of Paleolimnology* 44: 51–67.

Dragone F, Maino A, Malatesta A and Segre AG (1967) *Note illustrative del Foglio 149 Cerveteri della Carta Geologica d'Italia.* Roma: Servizio Geologico d'Italia.

Fouache E and Pavlopoulos K (2005) Sea-level changes in eastern Mediterranean during Holocene: Indicators and human impacts. *Zeitschrift für Geomorphologie* 137: Supplementary Issue.

Galloway WE (1975) Process framework for describing the morphologic and stratigraphic evolution of deltaic depositional system. In: Broussard ML (ed.) *Deltas, Models for Exploration.* Houston: Geological Society, 87–98.

Giraudi C (2002) Evoluzione ambientale tardo-olocenica nell'area comprendente il sito eneolitico di Maccarese (Fiumicino). In: Manfredini A (ed.) *Le dune, il lago, il mare. Una comunità di villaggio dell'Età del Rame a Maccarese.* Firenze: Istituto Italiano di Preistoria e Protostoria, 25–35.

Giraudi C (2004) Evoluzione tardo-olocenica del delta del Tevere. *Il Quaternario* 17: 477–492.

Giraudi C, Paroli L, Ricci G and Tata C (2006) Portus (Fiumicino – Roma). Il colmamento sedimentario dei bacini del Porto di Claudio e Traiano nell'ambito dell'evoluzione ambientale tardo-antica e medievale del delta del Tevere. *Archeologia Medievale* 33: 49–60.

Giraudi C, Tata C and Paroli L (2009) Late Holocene evolution of Tiber River Delta and geoarchaeology of Claudius and Trajan Harbor, Rome. *Geoarchaeology* 24(3): 371–382.

Giusti F and Castagnolo L (1982) I molluschi terrestri delle dune italiane: Brevi cenni di ecologia, elenco delle specie e chiavi per il loro riconoscimento. In: CNR (ed.) *Quaderni 'Struttura delle zoocenosi terrestri'. 3. Ambienti mediterranei. 1. Le coste sabbiose.* Roma: AQ/1/172-180, 51–102.

Goiran JP, Ognard C, Tronchère H, Canterot X and Cluze JA (2007) Recent geo-archeological findings of Portus, the ancient Harbour of Rome. In: Cinque A (ed.) *Abstracts of International Congress on People/Environment Relationships from Mesolithic to Middle Ages: Recent Geo-Archaeological Findings in Southern Italy.* Salerno 4–7 September 2007, Università di Napoli 'Federico I', 30–31.

Goiran JP, Tronchère H, Collalelli U, Salomon F and Djerby H (2009a) Decouvert d'un niveau marin biologique sur les quais de Portus: Le port antique de Rome. *Méditerranée* 112: 59–67.

Goiran JP, Tronchère H, Salomon F, Carbonel P, Djerbi H and Ognard C (2009b) Paleoenvironmental recontruction of the ancient harbors of Rome: Claudius and Trajan's marine harbors on the Tiber delta. *Quaternary International* 216: 3–13.

Isaja P and Lattanzi V (1992) *In ore Tiberis.* Roma: Cooperativa Ricerca sul Territorio.

Keay S, Millett M, Paroli L and Strutt K (2005) *Portus: An Archaeological Survey of the Port of Imperial Rome.* Roma: Archaeological Monographs of the British School at Rome.

Kerney MP and Cameron RAD (1979) *A Field Guide to the Land Snails of Britain and North-west Europe.* London: Collins.

Kukavicic M and Pranzini E (2003) Beach ridges and dunes of the Arno River delta. In: Ozhan E (ed.) *Proceeding of the Sixth International Conference on the Mediterranean Coastal Environment. Medcoast 03.* Ravenna 7–11 October 2003, MEDCOAST Secretariat, 1413–1424.

Lambeck K, Anzidei M, Antonioli F, Benini A and Esposito A (2004) Sea level in Roman time in the central Mediterranean and implication for recent change. *Earth and Planetary Science Letters* 224: 563–575.

Lanciani R (1888) Il campus salinarum romanarum. *Bollettino Commissione Archeologica Comunale di Roma* 16: 83–91.

Lanciani R (1903) Le antichità del territorio Laurentino. *Monografie Antiche* 13.

Limaye RB, Kumaran KPN, Nair KM and Padmalal D (2007) Non-pollen palynomorphs (NPP) as potential palaeoenvironmental indicators in the Late Quaternary sediments of west coast of India. *Current Science* 92: 1370–1382.

Lirer F, Sprovieri M, Ferraro L, Vallefuoco M, Cascella A, Petrosino P et al. (2009) High-resolution event stratigraphy for the last 10 kyr from the eastern Tyrrhenian margin sedimentary record. In: Atti Convegno (ed.) *La variabilità del clima nel Quaternario: la ricerca italiana.* Roma 18–20 febbraio 2009, Associazione Italiana per il QUAternario (AIQUA), 69–70.

Ložek V (1964) Quartärmollusken der Tschechoslowakei. *Rozpravy Ustredního Ustavu Geologického* 31: 1–368.

Lucchese F (1996) Duna litorale del rifugio WWF di Macchiagrande-Fregene. In: Dinelli A and Guarrera PM (eds) *Ambienti di particolare interesse naturalistico del Lazio, Censimento del patrimonio vegetale del Lazio.* Roma: Quaderno 2, Regione Lazio, 199–200.

Magri D and Sadori L (1999) Late Pleistocene and Holocene pollen stratigraphy at Lago di Vico (central Italy). *Vegetation History and Archaeobotany* 8: 247–260.

Manes F, Grignetti A, Tinelli A, Lenz R and Ciccioli P (1997) General features of the Castelporziano test site. *Atmosphere Environment* 31: 19–25.

Marriner N and Morhange C (2006) The 'Ancient Harbour Parasequence': Anthropogenic forcing of the stratigraphic highstand record. *Sedimentary Geology* 186: 13–17.

Marriner N and Morhange C (2007) Geoscience of ancient Mediterranean harbours. *Earth Science Reviews* 80: 137–194.

Mayewski PA, Rohling EE, Stager JC, Karlén W, Maasch KA, Meeker LD et al. (2004) Holocene climate variability. *Quaternary Research* 62: 243–255.

Mercuri AM, Accorsi CA and Bandini Mazzanti M (2002) The long term history of *Cannabis* and its cultivation by Romans in central Italy, shown by pollen records from Lago Albano and Lago di Nemi. *Vegetation History and Archaeobotany* 11: 263–276.

Morelli C, Olcese G and Zevi F (2004) Scoperte recenti sulle saline portuensi (*Campus salinarum romanarum*) e un progetto di ricerca sulla ceramica dell'area ostiense in età repubblicana. In: Zevi AG and Turchetti R (eds) *Méditerranée occidentale antique les échanges.* Marseille: ANSER Project III seminario, 43–55.

Morhange C, Blanc F, Bourcier M, Carbonel P, Prone A, Smitt-Mercury S et al. (2003) Bio-sedimentology of the late-Holocene deposits of the ancient harbour of Marseilles (southern France Mediterranean sea). *The Holocene* 13: 593–604.

Oberholtzer F (1875) *Le foci del Tevere.* Roma: Tipografia G.B. Paravia & Comp.

Pantaléon-Cano J, Yll EI, Pèrez-Obiol R and Roure JM (2003) Palynological evidence for vegetational history in semiarid areas of the western Mediterranean (Almerìa, Spain). *The Holocene* 13: 109–119.

Pérès JM and Picard J (1964) Nouveau manuel de Bionomie benthique de la Mer Méditerranée. *Recueil des Travaux de la Station Marine d'Endoume Bulletin* 31(47): 5–137.

Prahl FG, Bennett JJ and Carpenter R (1980) The early diagenesis of haliphatic hydrocarbons and organic matter in sedimentary particulates from Dabob bay, Washington. *Geochimica Cosmochimica Acta* 44: 1967–1976.

Principe C, Malfatti A, Rosi M, Ambrosio M and Fagioli MT (1997) Metodologia innovativa di carotaggio microstratigrafico: Esempio di applicazione alla tefrostratigrafia di prodotti vulcanici distali. *Geologia Tecnica & Ambientale* 4: 39–50.

Ramsey B (2005) O*xcal V.3.10.* Oxford: Research Laboratory for Archaeology.

Reille M (1992) *Pollen et spores d'Europe et d'Afrique du Nord.* Marseille: Laboratoire de Botanique Historique et Palynologie, URA CNRS 1152.

Reille M (1995) *Pollen et spores d'Europe et d'Afrique du Nord.* Marseille: Laboratoire de Botanique Historique et Palynologie, URA CNRS 1152 Supplement 1.

Reille M (1998) *Pollen et spores d'Europe et d'Afrique du Nord.* Marseille: Laboratoire de Botanique historique et Palynologie, URA CNRS 1152 Supplement 2.

Reinhardt EG, Patterson RT, Blenkisop J and Raban A (1998) Paleoenvironmental evolution of the inner basin of the ancient harbour at Cesarea Maritima, Israel; foraminiferal and Sr isotopic evidence. *Revue de Paleontologie* 17: 1–21.

Rendell HM, Claridge AJ and Clarke ML (2007) Late Holocene Mediterranean coastal change along Tiber Delta and Roman occupation of the Laurentine shore, central Italy. *Quaternary Geocronology* 2: 83–88.

Roy PS, Williams RJ, Jones AR, Yassini R, Gibbs PJ, Coates B et al. (2001) Structure and function of south-east Australian estuaries. *Estuarine, Coastal and Shelf Science* 53: 351–384.

Sadori L, Giardini M, Giraudi C and Mazzini I (2010) The plant landscape of the imperial harbour of Rome. *Journal of Archaeological Science* 37: 3294–3305.

Scott L (1992) Environmental implications and origin of microscopic *Pseudoschizaea* Thiergart and Frantz ex R. Potonié emend. in sediments. *Journal of Biogeography* 19: 349–354.

Stanley DJ (2005) Submergence and burial of ancient coastal sites on the subsiding Nile delta margin, Egypt. *Méditerranée* 104: 65–73.

Stanley DJ and Bernasconi MP (2006) Holocene depositional pattern and evolution in Alexandria's Eastern Harbor, Egypt. *Journal of Coastal Research* 22: 283–297.

Stanley DJ and Bernasconi MP (2009) Sybaris-Thuri-Copia trilogy: Three delta coastal sites become land-locked. *Méditerranée* 112: 75–88.

Stuiver M and Polach HA (1972) Discussion: Reporting of 14C data. *Radiocarbon* 19: 355–363.

van Geel B (1986) Application of fungal and algal remains and other microfossils in palynological analyses. In: Berglund BE (ed.) *Handbook of Holocene Palaeoecology and Palaeohydrology.* Chichester: Wiley, 497–506.

Vella C, Fleury TJ, Raccasi G, Provansal M, Sabatier F and Bourcier M (2005) Evolution of the Rhône Delta Plain in the Holocene. *Marine Geology* 222–223: 235–265.